ISSN 1070-3284, Russian Journal of Coordination Chemistry, 2019, Vol. 45, No. 6, pp. 446–456. © Pleiades Publishing, Ltd., 2019.

DNA Binding Properties of Sc(III) Complexes Derived from Rare-Earth(III) Ions and Semicarbazone of 8-Hydroxyquinoline-2-Carbaldehyde

Y. C. Liu[a], *, Y. Y. Li[a], H. L. Qi[a], H. S. Hu[a], K. J. Zhang[a], R. X. Lei[a], J. N. Liu[a], and X. D. Zheng[a]

[a] *College of Chemistry and Chemical Engineering, Longdong University and FLUOBON Collaborative Innovation Center, Longdong University, Qingyang, Gansu, 745000 P.R. China*

**e-mail: liuyc@ldxy.edu.cn*

Received May 7, 2018; revised June 26, 2018; accepted November 21, 2018

Abstract—The complex $[ScL_2(NO_3)]_2$ was prepared by $Sc(NO_3)_3 \cdot 6H_2O$ with 2-[(8-hydroxyquinolinyl)methylene]hydrazinecarboxamide (LH), and characterized by X-ray structure analysis (CIF file CCDC no. 1502531), where ligand L acts as a tetradentate ligand, binding to Sc(III) through the phenolate oxygen atom, nitrogen atom of quinolinato unit, the C=N group and O=C(NH_2)–N– group, and forming a Sc(III) complex with 1 : 2 metal to ligand stoichiometry, also forming two almost orthogonal ligand planes by eight-coordination at Sc(III) center with geometry of double-capped triangular prism. In addition, one free nitrate ion as charge-balance anion is found in the crystal cell. Then a series of rare-earth(III) complexes were prepared by $M(NO_3)_3 \cdot 6H_2O$ with ligand LH, where M(III) = Y, La, Ce, Pr, Nd, Sm, Eu, Gd, Tb, Dy, Ho, Er, Tm, Yb and Lu, and their DNA binding properties were investigated. It's found that these rare-earth(III) complexes could bind strongly to calf thymus DNA (CT-DNA) by the mode of intercalation with the binding constants at 10^4–10^5 M^{-1}, compared to ethidium bromide (EB), especially Sc(III) and Gd(III) complexes present stronger DNA binding properties than the others, while ligand LH presented a higher DNA binding property than its complexes. Moreover, cell cytotoxicity assay showed that uterine cervix carcinoma cell line (HeLa) presented low viabilities in the present of LH and representative complexes, and a concentration dependence, especially LH presents a higher inhibitory ability on HeLa cell viability than its complexes at lower concentration, which is consistent with the results of their DNA binding abilities.

Keywords: rare earth metal complexes, Sc(III) complex, X-ray crystallography, calf thymus DNA (CT-DNA), intercalation, cell cytotoxicity

DOI: 10.1134/S1070328419060034

INTRODUCTION

Previously, a series of neutral rare-earth(III) complexes were prepared from parts of rare earth ions M(III) and monad tetradentate ligands synthesized by the condensation reaction of 8-hydroxyquinoline-2-carboxaldehyde with benzoylhydrazine, 2-hydroxybenzoylhydrazine, 4-hydroxybenzoylhydrazine, and isonicotinylhydrazine, respectively. Then, their structures were characterized and DNA binding properties were investigated [1–12]. It's found that these rare-earth(III) complexes have similar structures and present stronger bindings to DNA through intercalation. All of them can form a binuclear rare-earth(III) complex with 1 : 1 metal to ligand stoichiometry by nine-coordination at rare-earth(III) center with geometry of distorted edge-sharing mono-capped square-antiprism of $[M^{III}(L)(NO_3)(DMF)_2]_2$ (M(III) = Y, La, Pr, Nd, Sm, Eu, Tb, Dy, Ho, Er) except for Yb(III) by eight-coordination at Yb(III) center with geometry of distorted edge-sharing dodecahedron of $[Yb(L)(NO_3)(DMF)]_2$. Additionally, these rare-earth(III) complexes can bind strongly to calf thymus DNA by the mode of intercalation compared to ethidium bromide (EB, K_b(EB–DNA) = 0.3068×10^5 M^{-1}), with the binding constants K_b = 0.8659–285.3 × 10^5 M^{-1}, and probably be used as potential antitumor drugs. However, all of aroylhydrazone side chain groups of O=C(C_6H_5)–NH– of ligands have enolized and deprotonated into $^-$O–C(C_6H_5)=N– after the formation of complexes, which induces a series of neutral charge and non-electrolyte rare-earth(III) complexes acting as little solubilities in water, though they can be dissolved in DMF or DMSO for further pharmacological examination.

Albrecht group [13] synthesized 2-[(8-hydroxyquinolinyl)methylene]hydrazinecarboxamide (LH) that is an effective tetradentate ligand for the coordination of rare-earth(III) ions. Investigations with yttrium(III) and lanthanum(III) in solution and in the solid state show that the small yttrium ion can form

2 : 2 (1 : 1 stoichiometry) and 2 : 1 ligand to metal complexes (X-ray structures: $[LY(NO_3)(DMF)_2]_2Cl_2 \cdot 2DMF$ and $[LL'Y] \cdot 3MeOH \cdot Et_2O$), where ligand L' is the enolized and deprotonated form of semicarbazone side chain in formation of complexes. With the larger lanthanum(III) ion only a well-defined 1 : 1 complex (X-ray structure: $[LLa(NO_3)\text{-}(MeOH)_2]_2\text{-}(NO_3)_2$) can be observed but probably 2 : 1 complexes are also formed. The X-ray structure analyses of $[(LH)MCl_3] \cdot MeOH$ (M = Er, Ho) and $Na[(\mu\text{-}NO_3)\{LEu(NO_3)_2\}_2] \cdot 2DMF$ show different coordination modes of the ligand. In view of the probably ionic form and better solubilities in water, in this study a series of rare-earth(III) complexes will be prepared from rare-earth(III) ions and ligand of LH referred as the literature [13]. Then their DNA binding properties will be investigated.

EXPERIMENTAL

Materials. Calf thymus DNA (CT-DNA), 8-hydroxyquinoline-2-carboxaldehyde and EB were obtained from Sigma-Aldrich Biotech. Co., Ltd. The stock complex solution (1.0 mM) of the investigated compound was prepared by dissolving the powdered material into appropriate amounts of 1 : 1 dimethylformamide (DMF) to H_2O solution for further investigation, while in cytotoxicity assay, 1.0 mM stock complex solution was prepared by dissolving the powdered material into appropriate amounts of 1 : 1 dimethylsulfoxide (DMSO) to H_2O solution. Deionized double distilled water and analytical grade reagents were used throughout. CT-DNA stock solution was prepared by dissolving the solid material in 5 mM Tris-HCl buffer (pH 7.20) containing 50 mM NaCl. The CT-DNA concentration in terms of base pair L^{-1} was determined spectrophotometrically by employing an extinction coefficient (ε) of 13200 L mol^{-1} cm^{-1} (base pair)$^{-1}$ at 260 nm and the concentration in terms of nucleotide L^{-1} was also determined spectrophotometrically by employing ε of 6600 L mol^{-1} cm^{-1} (nucleotide)$^{-1}$ at 260 nm [14]. The CT-DNA stock solution was stored at −20°C until it was used. EB was dissolved in 5 mM Tris-HCl buffer (pH 7.20) containing 50 mM NaCl and its concentration was determined assuming a molar extinction coefficient of 5600 L mol^{-1} cm^{-1} at 480 nm [15]. Uterine cervix carcinoma cell line (HeLa) was purchased from the Biology Preservation Center in Shanghai and cultured with DMEM medium (Gibco) supplemented with 10% fetal bovine serum (Gibco), 2 mM l-glutamine, 100 units/mL penicillin and 100 mg/mL streptomycin and incubated at 37°C in a humidified atmosphere of 5% CO_2 and 95% air.

Methods. The melting points of the compounds were determined on an XT4-100X microscopic melting point apparatus (Beijing). The IR spectra were recorded on a Nicolet Nexus 670 FT-IR spectrometer using KBr disc in the 4000–400 cm^{-1} region. ESI-MS (ESI-Trap/Mass) spectra were recorded on a Bruker Esquire 6000 mass spectrophotometer. Molar conductance of compound was tested using 1.0 mM stock solution.

Viscosity titration experiments were carried on an Ubbelohde viscometer in a thermostated water-bath maintained at 25.00 ± 0.01°C. Data were presented as $(\eta/\eta_o)^{1/3}$ versus the ratio of the compound to DNA, where η is the viscosity of DNA in the presence of the compound corrected from the solvent effect, and η_o is the viscosity of DNA alone [14, 16].

UV–Vis spectra were obtained using a Specord 50 (Analytik Jena) UV–Vis spectrophotometer with 1 cm quartz cell. The intrinsic binding constant *(K_b)* was determined by the following equation [17, 18]:

$$\frac{[DNA]}{\varepsilon_f - \varepsilon_a} = \frac{[DNA]}{\varepsilon_f - \varepsilon_b} + \frac{1}{K_b(\varepsilon_f - \varepsilon_b)}, \quad (1)$$

where [DNA] is the molar concentration of DNA in base pairs, ε_a corresponds to the extinction coefficient observed, ε_f corresponds to the extinction coefficient of the free compound, ε_b is the extinction coefficient of the compound when fully bound to DNA. The ratio of slope to intercept in the plot of $[DNA]/(\varepsilon_f - \varepsilon_a)$ versus [DNA] gives the values of K_b.

Fluorescence spectra were recorded using a RF-7000 spectrofluorophotometer (Hitachi) with 1 cm quartz cell. Both of the excitation and emission band widths were 10 nm. DNA–EB quenching assay was performed as the literatures [1–12]. DNA (4.0 μM, nucleotides) solution was added incrementally to 0.32 μM EB solution, then small aliquots of concentrated compound solutions (1.0 mM) were added till the drop-in fluorescence intensity (λ_{ex} = 525 nm, λ_{em} = 593 nm) reached a constant value. Measurements were made after 5 min at a constant water-bath temperature, 298 K. Stern–Volmer equation was used to determine the fluorescent quenching mechanism [19]:

$$F_o/F = 1 + K_{SV}[Q], \quad (2)$$

where F_o and F are the fluorescence intensity in the absence and in the presence of a compound at $[Q]$ concentration, respectively; K_{SV} is the Stern–Volmer dynamic quenching constant.

The cytotoxicity of compound on HeLa cell was measured by using MTT method in vitro. A suspension of cells (4000/well in 100 μL) were plated in 96-well plates and cultured for 12 h before addition of each compound. Then compounds ranging evenly from 20 to 80 μM were added to the corresponding plates. The plates were subsequently incubated for 24 h, the culture medium was removed and 100 μL of MTT solution (diluted in culture medium, 0.5 mg/mL) was added to each well. After 4 h of incu-

bation at 37°C, the MTT/medium was removed carefully and DMSO (100 μL) was added to each well to dissolve the formazan crystal. The absorbance of the wells was read by VICTOR^3 Multilabel Reader with a test wavelength of 490 nm. Cell viability was expressed as a percentage of control. All experiments were performed in triplicate.

Synthesis of LH was carried out referring to the literature [13]. The synthetic route for ligands LH and L'H is presented in Scheme 1. Productivity: 78.98%, melting point: 231–232°C. ESI-MS (DMF, *m/z*): 231.1044 [LH] · H^+. IR (KBr; ν_{max}, cm^{-1}): 3465 (N–H), 3387 (O–H), 1686 (C=O), 1603 (azomethine C=N), 1583 (pyridine C=N), 1327 (C–N), 1292 (C–OH). UV–Vis (DMF, λ_{max}, nm ($\varepsilon \times 10^4$, L mol^{-1} cm^{-1})): 285 (3.1216), 308 (1.7862). Λ_M, cm^2 Ω^{-1} mol^{-1} (DMF): 3.15.

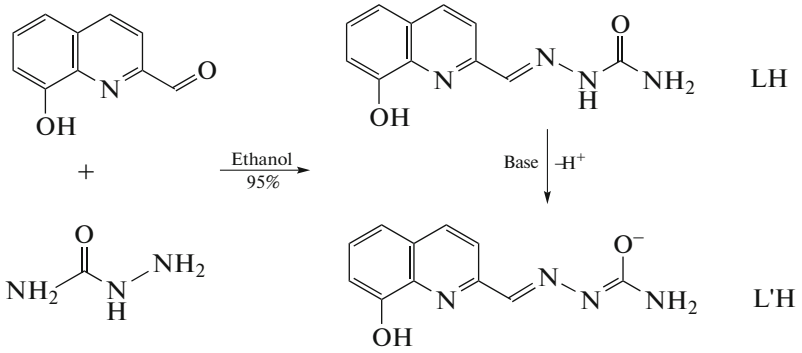

Scheme 1.

Synthesis of rare-earth(III) complexes were carried out by refluxing and stirring equimolar amounts of $M(NO_3)_3 \cdot 6H_2O$ (M = Sc^{3+}, Y^{3+}, La^{3+}, Ce^{3+}, Pr^{3+}, Nd^{3+}, Sm^{3+}, Eu^{3+}, Gd^{3+}, Tb^{3+}, Dy^{3+}, Ho^{3+}, Er^{3+}, Tm^{3+}, Yb^{3+}, Lu^{3+}) and a 30 mL methanol solution of ligand LH (0.046 g, 0.2 mmol) on a water bath, respectively. After refluxing for 30 min, triethylamine (0.020 g, 0.2 mmol) was added into the reaction mixture dropwise to deprotonate the phenolic hydroxyl substituent of 8-hydroxyquinolinato unit. Then the mixture was refluxed and stirred continuously for 8 h. After cooling to room temperature, the precipitate was centrifugalized, washed adequately with hot methanol and dried in vacuum over 48 h to give a powder, while the precipitate of a Sc(III) complex, $[ScL_2(NO_3)]$ (**I**) was obtained by vaporizing parts of solvent. The productivities were 62.0–75.6% and melting points exceed 300°C. The data of IR, UV–Vis, ESI-MS and Λ_M for these rare-earth(III) complexes were shown in Table 1.

X-ray structure determination. The orange transparent, X-ray quality crystal of I was obtained by vapor diffusion from its methanolic solution, where the complex was recrystllized in methanol suitable for X-ray measurements at room temperature for 3 days. The radiation used for a crystal was graphite-monochromated MoK_α radiation (λ = 0.71073 Å) and the data were collected on a Bruker APEX area-detector diffractometer by the ω–2θ scan technique at 298(2) K. The structure was solved by direct methods. All non-hydrogen atoms were refined anisotropically by full-matrix least-squares methods on F^2. Primary non-hydrogen atoms were found from direct methods and secondary non-hydrogen atoms were found from difference maps. The hydrogen atoms were added geometrically and their positions and thermal vibration factors were constrained. All calculations were performed using the programs SHELXS-97 and SHELXL-97 [20]. Crystal data and structure refinements for the X-ray structural analyses are presented in Table 2.

Supplementary material for structure **I** has been deposited with the Cambridge Crystallographic Data Centre (CCDC no. 1502531; deposit@ccdc.cam.ac.uk or http://www.ccdc.cam.ac.uk).

RESULTS AND DISCUSSION

All of the powdered complexes are orange and stable in air, compared with the characteristic IR bands between the powdered complexes and its ligand, it is found that phenolate oxygen atom, nitrogen atom of quinolinato unit, nitrogen atom of azomethine C=N and oxygen atom of semicarbazone O=C–NH– may participate in rare-earth(III) complexes. Additionally, the differences of typical bands ν_1 (N=O stretching vibration) and ν_2 (N–O antisymmetric stretching vibration) are greater than 115 cm^{-1}, meanwhile, $(\nu_3 + \nu_5) - (\nu_3 + \nu_6) \geq 25$ cm^{-1}, where bands of ν_3, ν_5, and ν_6 represent the symmetrical stretching vibration, antisymmetric stretching vibration and out of plane bending vibration of N–O, respectively, which indicates that nitrate ions bidentately participate in rare-earth(III) complexes except for **I**. However, free nitrate ions as charge-balance anions are found for all of the powdered complexes.

Table 1. The data of IR, UV-Vis, ESI-MS and Λ_M for rare-earth(III) complexes

Complex	IR (KB; ν_{max}, cm^{-1})														UV–Vis	ESI-MS	Λ_M
	N–H	C=N			NO_3^-							C–OM	O–M	N–M	λ_{max} nm ($\varepsilon \times 10^4$ L mol^{-1} cm^{-1})	*m/z*	cm^2 Ω^{-1} mol^{-1}
		azomethine	pyridine	free	$\nu_3 + \nu_5$, $\nu_3 + \nu_6$	ν_1 (N=O)	ν_2 AS	ν_3 SS	ν_4 SB	ν_5 AS	ν_6 PR						
Sc(III)	3447	1610	1597	1385		1474	1310			743		1275	570	470	307 (3.873), 361 (1.206)	503.1263 $[ScL_2]^+$	58.0
Y(III)	3437	1618	1589	1385	1772, 1735	1458	1310	1032	841	739	702	1273	569	482	307 (7.226), 361 (2.800)	546.9914 $[YL_2]^+$	124
La(III)	3447	1618	1595	1385	1794, 1735	1448	1310	1040	843	754	700	1273	559	484	288 (4.192), 307 (4.238)	596.9779 $[LaL_2]^+$	130
Ce(III)	3421	1618	1589	1385	1774, 1735	1456	1300	1011	839	766	733	1273	563	486	306 (6.452), 358 (1.198)	597.9781 $[CeL_2]^+$	170
Pr(III)	3421	1618	1589	1385	1774, 1735	1458	1302	1010	839	768	733	1273	561	486	309 (8.708), 359 (1.812)	598.9779 $[PrL_2]^+$	175
Nd(III)	3421	1622	1591	1385	1772, 1734	1456	1304	1011	839	768	719	1271	561	486	308 (6.378), 360 (1.352)	601.9949 $[NdL_2]^+$	137
Sm(III)	3431	1624	1591	1385	1774, 1750	1456	1312	1011	839	768	735	1271	563	488	307 (6.708), 361 (1.660)	609.9970 $[SmL_2]^+$	134
Eu(III)	3447	1618	1589	1385	1774, 1720	1458	1315	1014	839	758	702	1271	565	490	307 (6.192), 360 (1.696)	610.9993 $[EuL_2]^+$	115
Gd(III)	3447	1609	1589	1385	1772, 1717	1474	1315	1014	839	758	702	1271	565	492	269 (4.076), 305 (4.226)	615.9881 $[GdL_2]^+$	102
Tb(III)	3447	1618	1589	1385	1772, 1717	1458	1315	1013	839	758	702	1269	565	480	306 (7.356), 359 (2.444)	616.9516 $[TbL_2]^+$	150
Dy(III)	3441	1622	1589	1385	1774, 1717	1458	1313	1014	814	760	700	1267	567	480	306 (6.994), 360 (2.544)	621.9560 $[DyL_2]^+$	137
Ho(III)	3445	1622	1589	1385	1771, 1717	1458	1313	1013	839	760	702	1269	567	480	304 (6.752), 360 (2.380)	622.9541 $[HoL_2]^+$	121
Er(III)	3447	1610	1589	1385	1772, 1717	1458	1312	1013	839	758	702	1267	569	482	306 (6.752), 360 (2.238)	623.9531 $[ErL_2]^+$	145
Tm(III)	3438	1610	1589	1385	1772, 1720	1450	1312	1013	839	758	702	1273	569	480	308 (6.584), 360 (2.406)	626.9604 $[TmL_2]^+$	136
Yb(III)	3447	1610	1597	1385	1774, 1720	1458	1312	1013	841	758	702	1273	571	482	308 (5.570), 362 (2.124)	631.9639 $[YbL_2]^+$	123
Lu(III)	3421	1610	1589	1385	1774, 1717	1460	1312	1013	839	758	702	1273	571	482	308 (6.692), 361 (2.478)	632.9693 $[LuL_2]^+$	116

Table 2. Crystallographic data and structure refinement for complex $[ScL_2(NO_3)]_2$

Parameter	Value
Empirical formula	$C_{22}H_{18}N_9O_7Sc$
Formula weight	565.41
T, K	298(2)
Wavelength, Å	0.71073
Radiation	MoK_α
Crystal system	Monoclinic
Space group	*C2/m*
a, Å	14.9661(13)
b, Å	24.710(2)
c, Å	9.7410(9)
β, deg	118.690(3)
V, Å^3	3160.1(5)
Z	4
ρ_{calcd}, g cm^{-3}	1.188
μ, mm^{-1}	0.282
F(000)	1160
Crystal size, mm	0.30 × 0.21 × 0.10
$\theta_{min/max}$, deg	2.28–25.01
Index ranges	$-17 \le h \le 15$, $0 \le k \le 29$, $0 \le l \le 11$
Reflections collected/unique (R_{int})	2823/2823 (0.0000)
Completeness to θ = 25.01°, %	98.4
Absorption correction	Semi-empirical from equivalents
Max. and min. transmission	0.9723 and 0.9202
Refinement method	Full-matrix least-squares on F^2
Refinement parameters	181
Goodness-of-fit on F^2	0.991
Final R indices ($I > 2\sigma(I)$)	$R_1 = 0.0975$, $wR_2 = 0.1546$
R indices (all data)	$R_1 = 0.1833$, $wR_2 = 0.1733$
$\Delta\rho_{min}/\Delta_{max}$, e Å^{-3}	0.828/–0.406

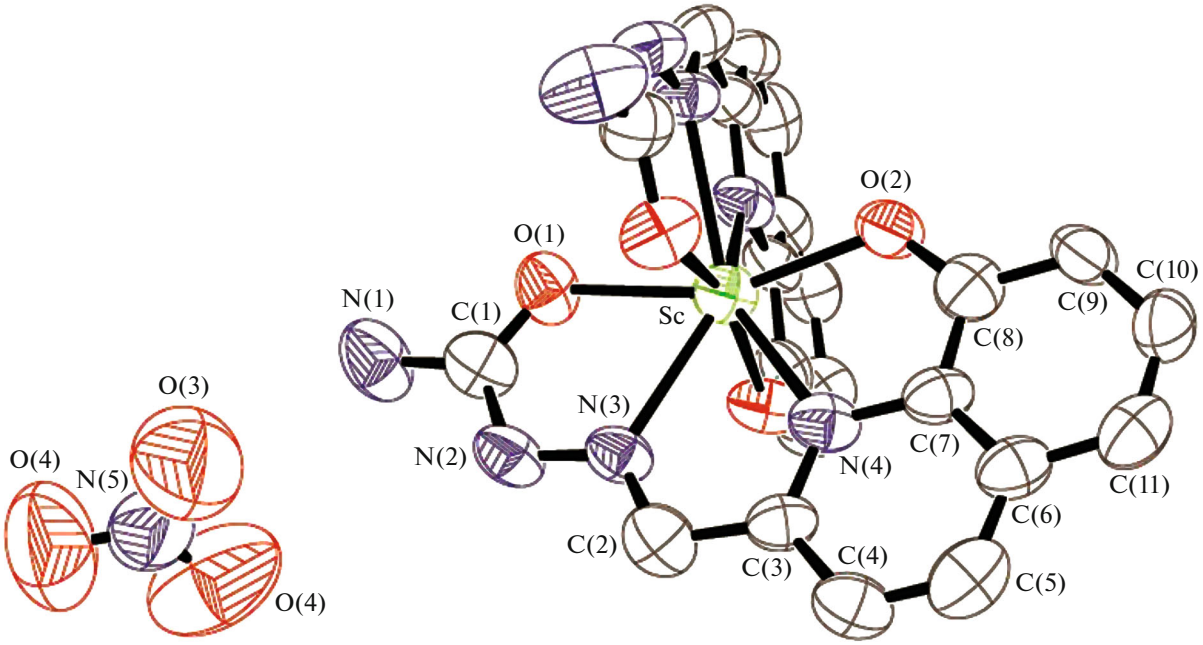

Fig. 1. The Ortep structure of X-ray crystal of $[ScL_2(NO_3)]$.

The melting points of all the powdered complexes exceed 300°C. They are easily soluble in 1 : 1 DMF to H_2O solution than either in DMF or H_2O alone. The molar conductivities Λ_M in 1 : 1 DMF to H_2O solution are 58.0–170 $cm^2\,\Omega^{-1}\,mol^{-1}$, indicating that they act as 1 : 1 electrolyte [21]. ESI-MS data show that the mainly stable components of complexes are $[ML_2]^+$ in 1 : 1 DMF to H_2O solution, though little fragments are present, such as $[ML']^+$, $[ML'(NO_3)]$, $[ML(NO_3)]^+$, [MLL'], $[(ML')_2(NO_3)]^+$, $[(M_2LL')_2(NO_3)_2]^+$, $[(ML')_2(NO_3)_2]$, etc., where O=C(NH_2)–NH– of semicarbazone side chain for ligand has partly enolized and deprotonated into $^-$O–C(NH_2)=N– as represented by L' [13].

Figure 1 shows the Ortep diagram of X-ray structure of **I**. Ligand L acts as a tetradentate ligand, binding to Sc(III) through the phenolate oxygen atom, nitrogen atom of quinolinato unit, the C=N and O=C(NH_2)–N– groups, and forming complex **I** with 1 : 2 metal to ligand stoichiometry with two almost orthogonal ligand planes by eight-coordination at Sc(III) center with geometry of double-capped triangular prism, where the band lengths of C(1)=O(1) (1.243(7)), C(1)–N(2) (1.335(7)) and N(2)–N(3) (1.364(6) Å) are not consistent with the normals (the normal band lengths of C=O, C–N, C–O, C=N (conjugated) and N=N are 1.19–1.23, 1.47–1.50, 1.30–1.39, 1.34–1.38 and 1.22–1.30 Å, respectively [22]). This indicates that the trends of semicarbazone side chain partly enolized and band lengths averaged are favorable when the ligand participate in rare-earth(III) complexes. Also, one free nitrate ion as charge-balance anion is found in the crystal cell. This X-ray structure of **I** is different from those of $[LY(NO_3)(DMF)_2]_2Cl_2 \cdot 2DMF$, $[LL'Y] \cdot 3MeOH \cdot Et_2O$), $[LLa(NO_3)(MeOH)_2]_2(NO_3)_2$), $Na[(\mu\text{-}NO_3)\text{-}\{LEu(NO_3)_2\}_2] \cdot 2DMF$ and $[(L\text{-}H)MCl_3] \cdot MeOH$ (M = Er, Ho) [13].

Comparison of the structural parameters of ligands LH binding to Sc(III), Y(III), and La(III) metal centers are listed in Table 3. It is found that with the size of metal center decreasing, the binding lengths of M–O and M–N decrease, while the binding angles of OMN and NMN increase.

Viscosity titration measurements were carried out to clarify the interaction modes between the investigated compounds and CT-DNA. Hydrodynamic measurements that are sensitive to length change of DNA (i.e., viscosity and sedimentation) are regarded as the least ambiguous and the most critical criterions for binding modes in solution in absence of crystallographic structural data, as viscosity is proportional to the cube of length L of rod-like DNA [15, 23]. Intercalation involves the insertion of a planar molecule between DNA base pairs, resulting in a decrease in the DNA helical twist and lengthening of the DNA, therefore intercalators cause the unwinding and lengthening of DNA helix as base pairs become separated to accommodate the binding compound [24]. Whereas, agents bound to DNA through groove binding do not alter the relative viscosity of DNA, and agents bound to DNA through electrostatic binding will bend or kink the DNA helix, reducing its effective length and

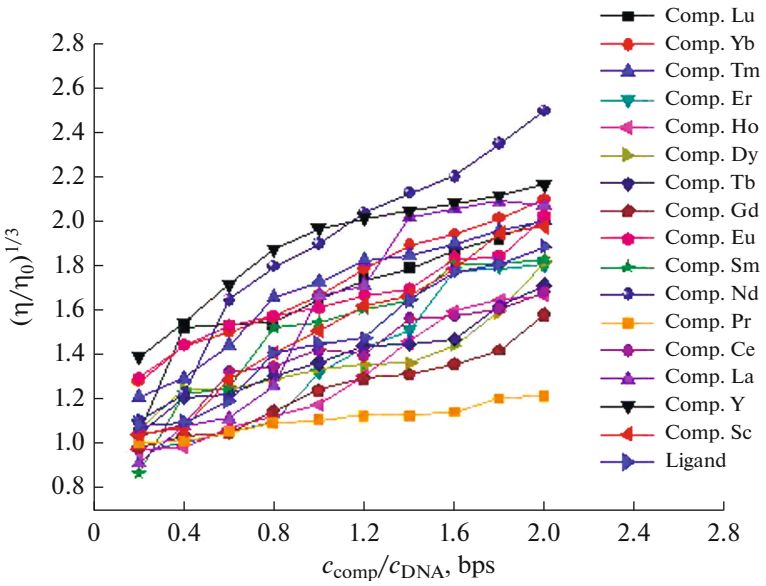

Fig. 2. Effects of increasing amounts of the investigated compounds on the relative viscosity of CT-DNA in 5 mM Tris-HCl buffer solution (pH 7.20) containing 50 mM NaCl at 25.00 ± 0.01°C. The concentration of CT-DNA was 50 μM (bps).

its viscosity, concomitantly [16, 25]. With the ratio of the investigated compound to DNA (bps) increasing, the relative viscosity of DNA increases steadily as shown in Fig. 2, indicating that intercalation takes place between these compounds with DNA helix.

The UV–Vis absorption spectra of the investigated compounds in the absence and presence of the CT-DNA were obtained in DMF : Tris-HCl buffer (5 mM, pH 7.20) containing 50 mM NaCl of 1 : 100 solutions, respectively. The UV-Vis spectrum of ligand presents two typical bands of λ_{max} at 285 nm ($\varepsilon = 3.122 \times 10^4$) and 308 nm ($\varepsilon = 1.786 \times 10^4$), while the UV–Vis spectra of complexes presents two typical bands of λ_{max} at 269–309 nm ($\varepsilon = 3.873–8.708 \times 10^4$) and 305–361 nm ($\varepsilon = 1.198–4.238 \times 10^4$), respectively, which can be assigned to π–π* transition of conjugated aromatic rings and the charge transfer from ligand to metal ions ($L \rightarrow M^{3+}$) [26, 27]. Upon successive addition of CT-DNA (bps), the UV–Vis

Table 3. Comparison of the structural parameters of ligands LH binding to Sc(III), Y(III) and La(III) metal centers

Bond and angle	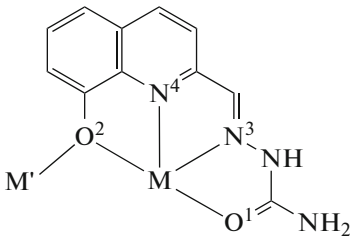		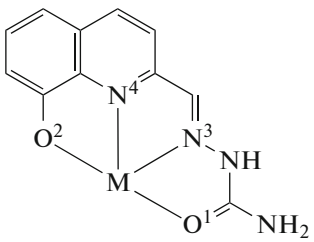
	$[LaL(NO_3)(MeOH)_2]_2(NO_3)_2$ [13]	$[YL(NO_3)(DMF)_2]_2Cl_2$ [13]	$[ScL_2(NO_3)]$
O(1)–M	2.414(3)	2.355(3)	2.236(4)
N(3)–M	2.620(4)	2.563(4)	2.378(5)
N(4)–M	2.541(3)	2.470(3)	2.303(5)
O(2)–M	2.425(3)	2.346(3)	2.109(4)
O(2)–M'	2.387(3)	2.354(3)	
O(2)MN(4)	65.5(1)	66.8(1)	71.65(19)
N(3)MN(4)	60.4(1)	61.4(1)	64.2(2)
O(1)MN(3)	60.9(1)	63.1(1)	66.82(18)
Distance between M···M'	3.980	3.886	

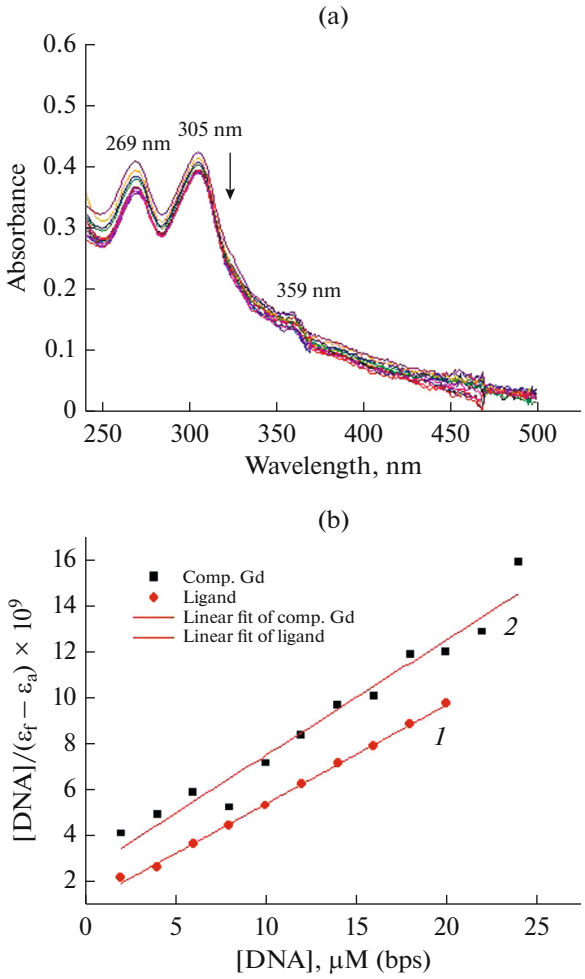

Fig. 3. (a) The UV–Vis spectra for Gd(III) complex upon successive addition of CT-DAN (similar to the other compounds); (b) the plots of [DNA]/(ε_f–ε_a) versus [DNA] for ligand (*1*) and its Gd(III) complex (*2*).

absorption bands of ligand and its metal complexes show progressive hypochromisms, indicating that the strong stacking interactions take place between the aromatic chromophores of the compounds and base pairs of DNA other than the non-covalently intercalative binding of compounds to DNA helix [28, 29] The magnitude of hypochromism is parallel to the intercalative strength and the affinity of a compound binding to DNA [23].

Figure 3 shows the UV–Vis spectra for Gd(III) complex upon successive addition of CT-DAN (similar to the other compounds) and the plots of [DNA]/(ε_f–ε_a) versus [DNA] for ligand and complex **I**, respectively. Then the binding constants (K_b = 1.754–32.49 × 10^4 M^{-1}) of DNA and the investigated compounds are determined and the values of K_b are listed in Table 4. Compared with EB (classical intercalative agent) binding to DNA ($K_{b\ (EB–DNA)}$ = 3.068 × 10^4 M^{-1} at the same experimental conditions [10], ligand LH and Sc(III) or Gd(III) complexes present higher binding abilities to DNA than EB, however, the other complexes are at the same magnitude of binding abilities as EB binding to DNA, mainly due to the size and electronic effects of metal ions. Moreover, ligand LH presents higher binding ability to DNA than its complexes, mainly due to the structurally steric hindrance effects of complexes. Additionally, although the binding ability of ligand LH to DNA is at the same magnitude as Schiff-baes ligands of 8-hydroxyquinoline-2-carboxaldehyde condensed with benzoylhydrazine, 2-hydroxybenzoylhydrazine, 4-hydroxybenzoylhydrazine and isonicotinylhydrazine, the DNA binding abilities of rare-earth complexes derived from ligand LH are generally weaker than complexes of derived from the latter four Schiff-baes ligands (K_b = 1.422–285.3 × 10^5 M^{-1}) [1–12], which are mainly due to the little group $-NH_2$ of ligand LH other than aromatic properties of phenyl or pyridine. Furthermore, the DNA binding abilities of rare-earth complexes derived from ligand LH are weaker than those of lanthanide-metal-ion complexes derived from 8-hydroxyquinoline-7-carboxaldehyde(isonicotinyl)hydrazone (K_b = 9.5–16.7 × 10^5 M^{-1}) and 8-hydroxyquinoline-7-carboxaldehyde(benzoylhydrazone (K_b = 2.938–26.13 × 10^5 M^{-1}) [30, 31], weaker than those derived from 3-carbaldehyde chromone with isonicotinyl hydrazine, 1-phenyl-3-methyl-4-formyl-2-pyrazolin-5-one (PMFP) with isonicotinyl hydrazine and PMFP with 4-aminophenazone, in which Ln(III) = La, Nd, Sm, Tb, Dy, Yb and K_b = 2.44–7.6 × 10^5 M^{-1} [32–34]. Also, they show weaker binding to CT-DNA than complex **I** derived from Congo red (CR) binding to herring sperm DNA, in which the K_b of Sm(III)$(CR)_3$ complex is 6.25 × 10^6 M^{-1} at 18°C and 1.11 × 10^7 M^{-1} at 26°C [35].

The fluorescence emission intensity of DNA-EB system decreased dramatically upon the increasing amounts of the ligand and its complexes. The fluorescent spectra of DNA–EB system upon successive addition of complex **I** (similar to those of the others) and the Stern–Volmer plots for ligand and its complexes in DNA–EB systems are shown in Fig. 4 and the data of Stern–Volmer quenching constants are collected in Table 4. The values of K_{SV} are 0.7583–84.35 × 10^4 M^{-1}. The loss of fluorescence intensity at the maximum wavelength indicates that most of the EB molecules have been displaced from DNA–EB complex by every quencher at the approximately saturated end point, which indicates further that the intercalative binding takes place between the investigated compound and DNA. Stern–Volmer quenching constant can also be interpreted as the association or binding constant of the complexation reaction [36]. Although ligand presents higher binding ability to DNA than its complexes, but it presents lower quenching constant than its complexes.

Table 4. Parameters of K_b, K_{SV} and FC_{50} for ligand and its rare earth metal complexes

Compound	K_b, 10^4 M^{-1}	K_{SV}, 10^4 M^{-1}	FC_{50}, μM ($c_{compound}/c_{DNA,\ nucleotides}$)
Ligand	32.49 ± 8.68	0.7583 ± 0.044	143.9 (17.98 : 1)
Sc(III)	29.57 ± 6.79	3.401 ± 0.259	36.41 (4.095 : 1)
Y(III)	1.754 ± 0.744	11.18 ± 2.07	13.52 (1.690 : 1)
La(III)	5.725 ± 0.587	1.461 ± 0.166	75.01 (9.376 : 1)
Ce(III)	1.900 ± 0.517	4.035 ± 0.144	27.92 (3.490 : 1)
Pr(III)	5.348 ± 0.517	6.068 ± 0.213	17.56 (2.195 : 1)
Nd(III)	2.658 ± 0.587	4.206 ± 0.492	27.06 (3.382 : 1)
Sm(III)	7.169 ± 0.515	3.120 ± 0.082	35.63 (4.454 : 1)
Eu(III)	1.822 ± 0.580	4.847 ± 0.277	25.47 (3.184 : 1)
Gd(III)	20.49 ± 6.79	84.35 ± 10.90	6.612 (0.8265 : 1)
Tb(III)	6.435 ± 0.709	3.726 ± 0.257	32.72 (4.089 : 1)
Dy(III)	11.85 ± 0.52	3.378 ± 0.154	36.19 (4.524 : 1)
Ho(III)	8.586 ± 0.501	3.688 ± 0.156	30.56 (3.820 : 1)
Er(III)	3.366 ± 0.587	3.024 ± 0.224	39.92 (4.990 : 1)
Tm(III)	3.101 ± 0.630	2.088 ± 0.084	55.54 (6.942 : 1)
Yb(III)	2.775 ± 0.545	1.683 ± 0.108	78.22 (9.777 : 1)
Lu(III)	6.456 ± 0.992	2.991 ± 0.185	37.11 (4.639 : 1)

On the other hand, it is well known that DNA is an anionic polyelectrolyte because of phosphate groups. Therefore, studying the fluorescence behavior of small molecules at different ionic strengths is considered as another important option to investigate possible DNA-molecules interaction mechanism [37]. The experiments were carried out by fixing the concentration of test compound and CT-DNA in Tris-HCl buffer with pH 7.20 while varying the concentration of NaCl from 0.1 to 0.5 mol L^{-1}. In case of electrostatic binding, the fluorescence intensity of DNA-molecules complex will be disturbed with the addition of increasing concentration of Na^+ due to competitive binding of Na^+ with phosphate groups of DNA [38]. In this assay, the emission intensity of test compounds–DNA-EB complex has hardly changed upon progressive addition of Na^+, indicating non-electrostatic binding of these compounds with DNA takes place.

More importantly, DNA intercalators have been used extensively as antitumor, antineoplastic, antimalarial, antibiotic, and antifungal agents [23]. There is a criterion for screening out antitumor drugs from others by DNA–EB fluorescent tracer method, i.e., a compound may be used as a potential antitumor drug if it causes a 50% loss of DNA–EB fluorescence intensity by fluorescent titration before the molar concentration ratio of the compound to DNA (nucleotides) does not overrun 100 : 1 [39]. FC_{50} value is introduced to denote the molar concentration of a compound that causes a 50% loss in the fluorescence intensity of DNA–EB system. According to the data of FC_{50} and the molar ratios of compounds to DNA as shown in Table 4, it is interesting that at FC_{50}, all the molar concentration ratios of the complexes to DNA (6.612–78.22 : 1) are under 100 : 1 except for ligand at 143.9 : 1, indicating that these complexes are probably used as potential antitumor drugs, especially Gd(III) complex.

The toxicological properties of ligand LH and its representative complexes including Sc(III), La(III), Gd(III) and Yb(III) on HeLa cell were measured by using MTT method in vitro, respectively. Figure 5 shows the cell viability (100% control) of uterine cervix carcinoma cell line HeLa versus concentration of ligand LH and representative complexes. It' found that HeLa cell presents low viabilities in the present of LH and representative complexes and a concentration dependence, especially LH presents a higher inhibitory ability on HeLa cell viability than complexes at lower concentration, which is consistent with the results of their DNA binding abilities.

ACKNOWLEDGMENTS

We thank Professor Baodui Wang, School of Chemistry and Chemical Engineering, Lanzhou University, for his work in monitoring toxicological properties of ligand LH and its representative complexes on HeLa cell.

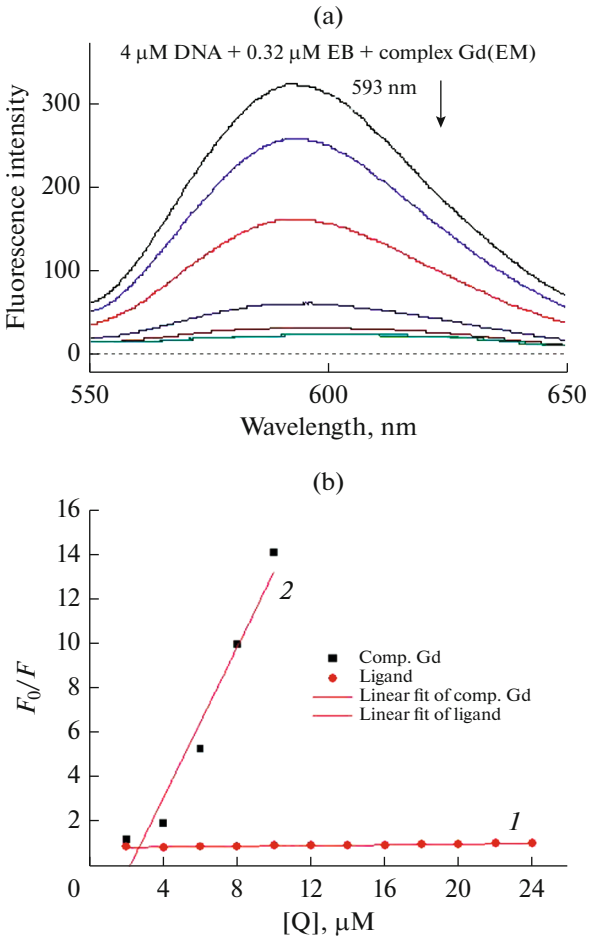

Fig. 4. (a) The fluorescent spectra of DNA-EB system upon successive addition of Gd(III) complex (similar to those of the others); (b) the Stern-Volmer plots for ligand (*1*) and its Gd(III) complex (*2*) in EB-DNA systems. λ_{ex} = 525 nm, λ_{em} = 593 nm, 298 K. The concentration of DNA is 4.0 μM (nucleotides) and the concentration of EB is 0.32.

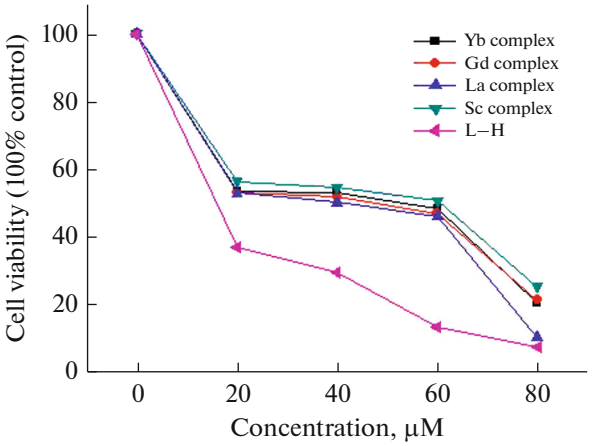

Fig. 5. The cell viability (100% control) of uterine cervix carcinoma cell line (HeLa) versus concentrations of ligand LH and representative complexes including Sc(III), La(III), Gd(III), and Yb(III).

FUNDING

The study was supported by Longdong University Doctor Fund (nos. XYZK1619, XYBY1501 and XYBY140210), Gansu Applied Chemistry Key Subject Fund (no. GSACKS20130113) and Fund of Longdong Advantageous Resources and Environmental Technology Collaborative Innovation Team (no. 2018c-22).

REFERENCES

1. Liu, Y.C. and Yang, Z.Y., *BioMetals*, 2009, vol. 22, p. 733.
2. Liu, Y.C. and Yang, Z.Y., *J. Org. Chem.*, 2009, vol. 694, p. 3091.
3. Liu, Y.C. and Yang, Z.Y., *J. Inorg. Biochem.*, 2009, vol. 103, p. 1014.
4. Liu, Y.C. and Yang, Z.Y., *Inorg. Chem. Commun.*, 2009, vol. 12, p. 704.
5. Liu, Y.C. and Yang, Z.Y., *Eur. J. Med. Chem.*, 2009, vol. 44, p. 5080.
6. Liu, Y.C., Jiang, X.H., Yang, Z.Y., et al., *Appl. Spectrosc.*, 2010, vol. 64, p. 980.
7. Liu, Y.C. and Yang, Z.Y., *J. Biochem.*, 2010, vol. 147, p. 381.
8. Liu, Y.C., Yang, Z.Y., Zhang, K.J., et al., *Aust. J. Chem.*, 2011, vol. 64, p. 345.
9. Liu, Y.C., Xu, X.Y., Lei, R.X., et al., *Chem. Res. Appl.* (in Chinese), 2013, vol. 25, p. 1475.
10. Liu, Y.C., Li, Y.Y., Qi, H.L., et al., *J. Coord. Chem.*, 2014, vol. 67, p. 3689.
11. Lei, R.X., Ma, D.P., Wei, X.X., et al., *Medicine Sciences and Bioengineering*, Wang, M., Ed., London: Taylor & Francis Group, 2015, p. 783.
12. Liu, Y.C., Li, Y.Y., Qi, H.L., et al., *Koord. Khim.*, 2017, vol. 43, no. 7, p. 434.
13. Albrecht, M., Osetska, O., and Frohliich, R., *Dalton Trans.*, 2005, vol. 23, p. 3757.
14. Zsila, F., Bikádi, Z., and Simonyi, M., *Org. Biomol. Chem.*, 2004, vol. 2, p. 2902.
15. Suh, D. and Chaires, J.B., *Bioorgan. Med. Chem.*, 1995, vol. 3, p. 723.
16. Satyanarayana, S., Dabrowiak, J.C., and Chaires, J.B., *J. Biochem.*, 1992, vol. 31, p. 9319.
17. Wolfe, A., Shimer, G.H., and Meehan, T., Jr., *J. Biochem.*, 1987, vol. 26, p. 6392.
18. Xi, P.X., Xu, Z.H., Liu, X.H., et al., *Spectrochim. Acta, A*, 2008, vol. 71, p. 523.
19. Ayar, A. and Mercimek, B., *Process Biochem.*, 2006, vol. 41, p. 1553.
20. Sheldrick, G.M., *Acta Crystallogr., Sect. A: Found. Crystallogr.*, 1990, vol. 46, p. 467.
21. Geary, W.J., *Coord. Chem. Rev.*, 1971, vol. 7, p. 81.
22. Chen, X.M. and Cai, J.W., *Single-Crystal Structural Analysis. Principles and Practices*, Beijing: Science, 2003.
23. Sigman, D.S., Mazumder, A., and Perrin, D.M., *Chem. Rev.*, 1993, vol. 93, p. 2295.

24. Palchaudhuri, R. and Hergenrother, P.J., *Curr. Opin. Biotech.*, 2007, vol. 18, p. 497.
25. Wang, B.D., Yang, Z.Y., Crewdson, P., and Wang, D.Q., *J. Inorg. Biochem.*, 2007, vol. 101, p. 1492.
26. Ismail, T.M.A., *J. Coord. Chem.*, 2005, vol. 58, p. 141.
27. Moawad, M.M. and Hanna, W.G., *J. Coord. Chem.*, 2002, vol. 55, p. 439.
28. Barton, J.K., Danishefsky, A.T., and Goldberg, J.M., *J. Am. Chem. Soc.*, 1984, vol. 106, p. 2172.
29. Lu, H.L., Liang, J.J., Zeng, Z.Z., et al., *Transition Met. Chem.*, 2007, vol. 32, p. 56.
30. Liu, Y.C., Zhang, K.J., Lei, R.X., et al., *J. Coord. Chem.*, 2012, vol. 65, p. 2041.
31. Liu, Y.C., Zhang, K.J., Wu, Y., et al., *Chem. Biodivers.*, 2012, vol. 9, p. 1533.
32. Li, Y. and Yang, Z.Y., *J. Coord. Chem.*, 2010, vol. 63, p. 1960.
33. Wang, M.F., Yang, Z.Y., Li, Y., and Li, H.G., *J. Coord. Chem.*, 2011, vol. 64, p. 2974.
34. Wang, M.F., Yang, Z.Y., Liu, Z.C., et al., *J. Coord. Chem.*, 2012, vol. 65, p. 3805.
35. Pan, H.Z., Wang, X.M., Li, H.B., et al., *J. Coord. Chem.*, 2010, vol. 63, p. 4347.
36. Bagatolli, L.A., Kivatinitz, S.C., and Fidelio, G.D., *J. Pharm. Sci.*, 1996, vol. 85, p. 1131.
37. Nayab, P.S., Akrema Ansari, I.A., et al., *Lumin.*, 2017, vol. 32, p. 829.
38. Gao, C., Liu, S., Zhang, X., et al., *Spectrochim. Acta, A*, 2016, vol. 156, p. 1.
39. Li, Z.L., Chen, J.H., Zhang, K.C., et al., *Sci. China, B*, 1991, vol. 21, p. 1193.